

Supplementary Materials for

Photonic paper: Multiscale assembly of reflective cellulose sheets in *Lunaria annua*

G. Guidetti, H. Sun, B. Marelli, F. G. Omenetto*

*Corresponding author. Email: fiorenzo.omenetto@tufts.edu

Published 1 July 2020, *Sci. Adv.* **6**, eaba8966 (2020)

DOI: [10.1126/sciadv.aba8966](https://doi.org/10.1126/sciadv.aba8966)

This PDF file includes:

Figs. S1 to S7

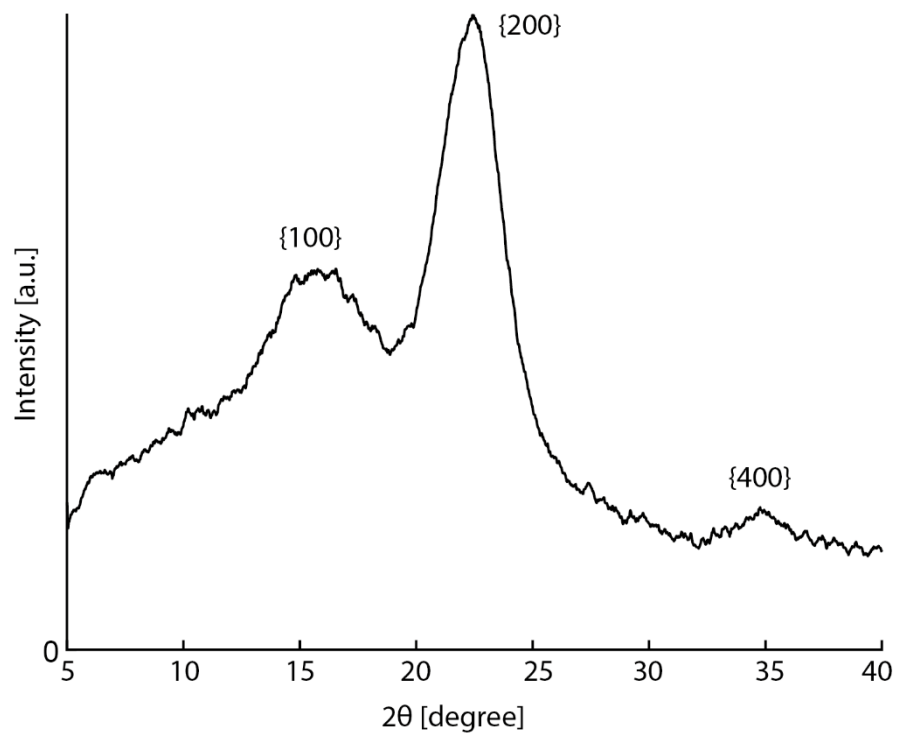


Fig. S1. X-ray diffraction plot of a *Lunaria annua* septum. The crystalline structure of the cellulose in the septum is cellulose I. This is confirmed by the peak positions of the crystalline family planes {100}, {200}, and {400} which are, respectively, at $2\theta \sim 14-17^\circ$, $\sim 22^\circ$, and 34° .

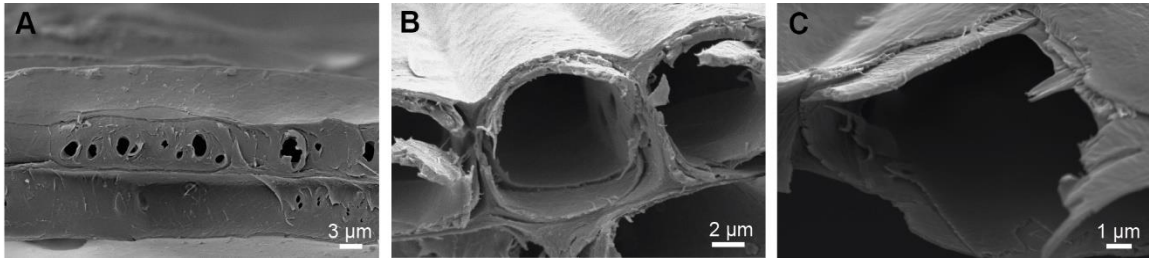


Fig. S2. Thin-film assembly in the *Lunaria* septum cells. The cellulose thin-film assembly in the cell wall can be seen in the delaminating bilayer construct (A) and in the cross-section of the cells (B) and (C). The cell wall pores can also be seen along the length of the cell in (A).

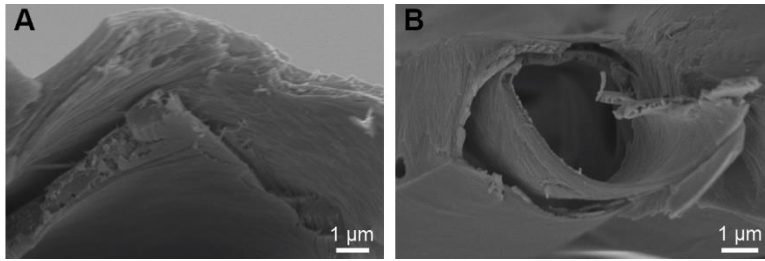


Fig. S3. Orientation of the cellulose fibers in the *Lunaria* cells' cladding. The cellulose fibers are seen aligning along the circumference of the thin film cladding constituting the cell wall.

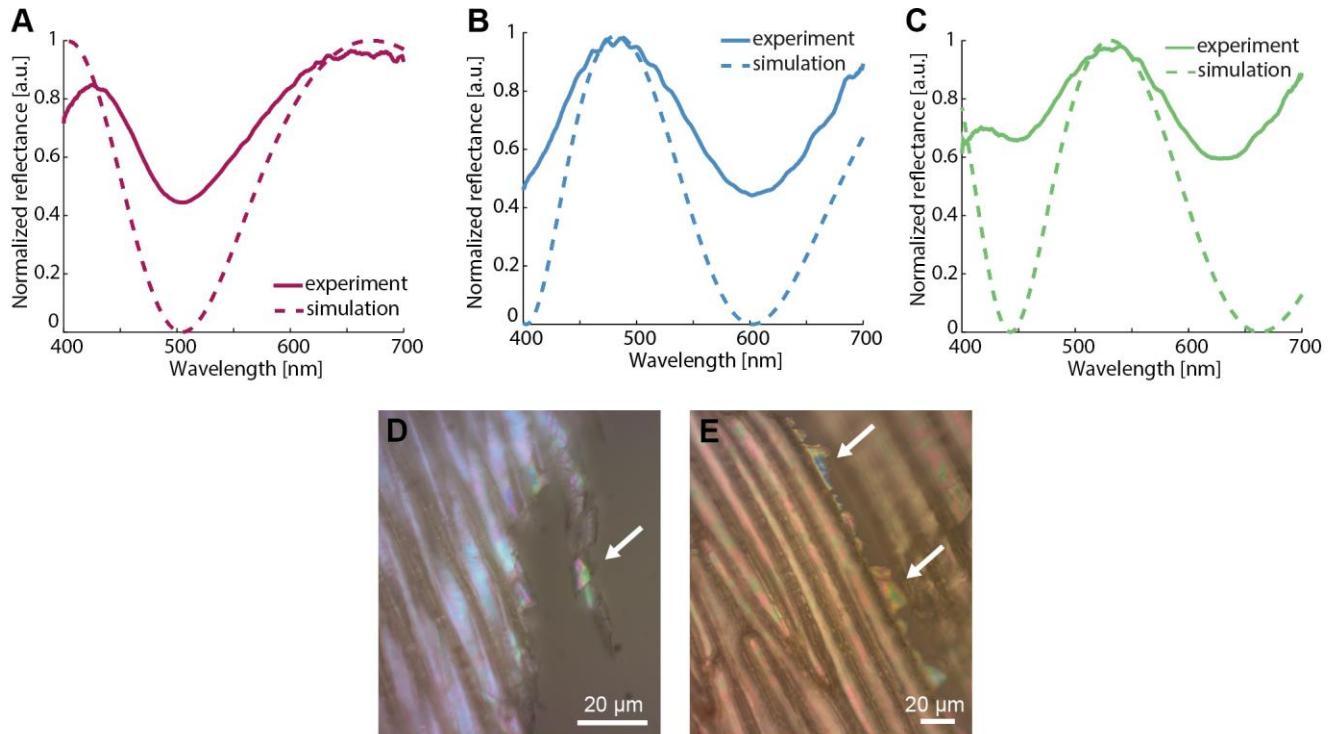


Fig. S4 Thin-film interference coloration in *Lunaria annua* septa. At the microscopic level the reflectance from individually colored regions consists in fringes caused by thin-film interference (solid lines). This behavior is confirmed by the reflectance spectrum (dashed lines) originated by simulating a 1D-thin film of cellulose surrounded by air which corresponds to the upper cladding of a single cell in the *Lunaria* septum. The experimental spectra reported in (A), (B) and (C) correspond, respectively, to the magenta, blue and green single-colored regions of Figure 2B. The simulated spectra reported in (A), (B) and (C) have been calculated using a cellulose thickness of, respectively, 318 nm, 380 nm, and 418 nm. (D) and (E) show macroscopic brightfield reflectance images of *Lunaria annua* septa where thin-film interference colors can be observed in delaminating regions of the cells (D, white arrow) and in broken parts of the cladding (E, white arrows).

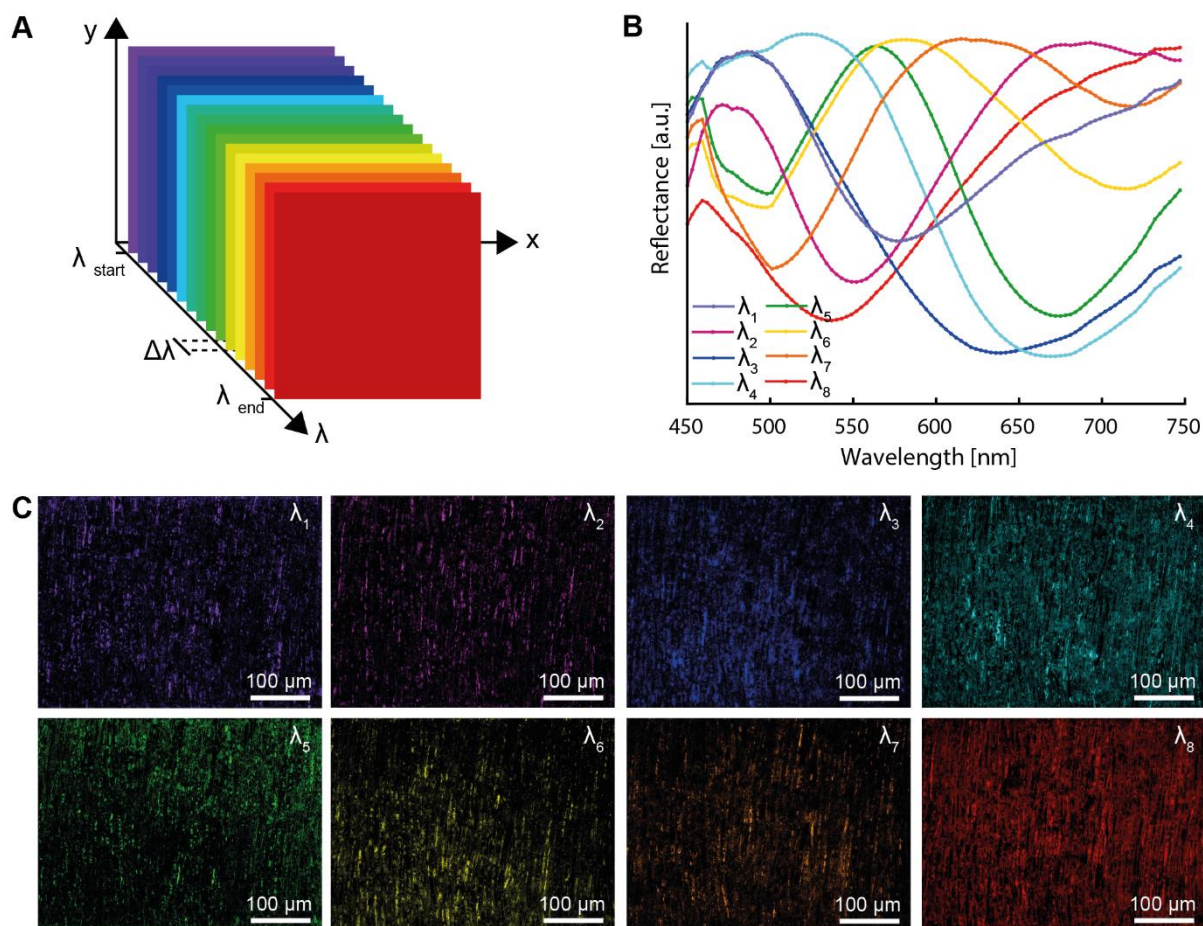


Fig. S5 Multispectral mapping of *Lunaria annua* septum. (A) Schematic representing the three-dimensional maps that can be obtained with a multispectral camera. The spectroscopic information of the sample, defined by the spatial coordinates x and y , is collected for each pixel at every wavelength defined by the range $\lambda_{\text{start}}-\lambda_{\text{end}}$ and by the step size $\Delta\lambda$. The stack of these images creates the three-dimensional map. (B) Reflectance spectra for 8 selected spectral bands corresponding to the main reflected colors from the *Lunaria* septum acquired in the spectral range 450-750 nm with a step size $\Delta\lambda = 3$ nm. (C) Corresponding false-color optical micrographs for each of the 8 selected spectral regions, showing the spatial localization of each reflected color.

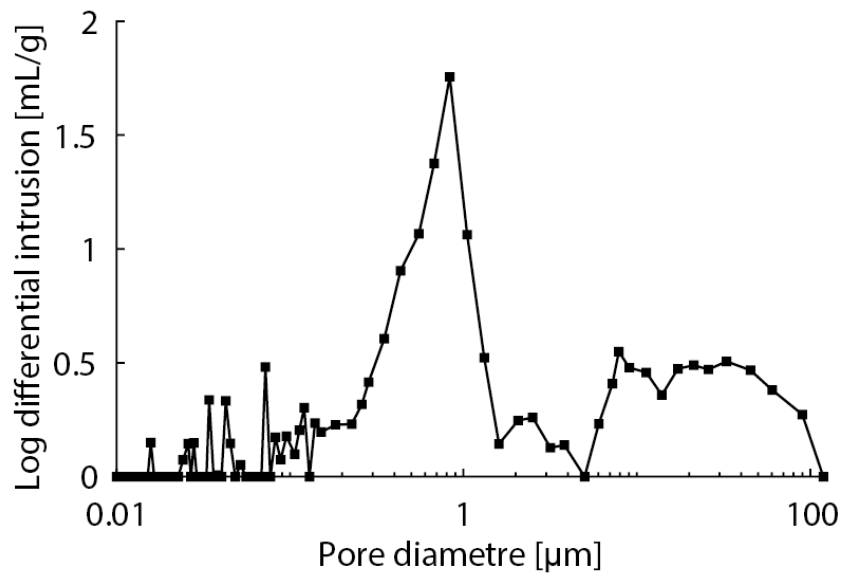


Fig. S6. Size distribution of the pores size in *Lunaria annua septa*. Pores diameter as determined using the Washburn equation corresponding to the cumulative intrusion data of Figure 3G.

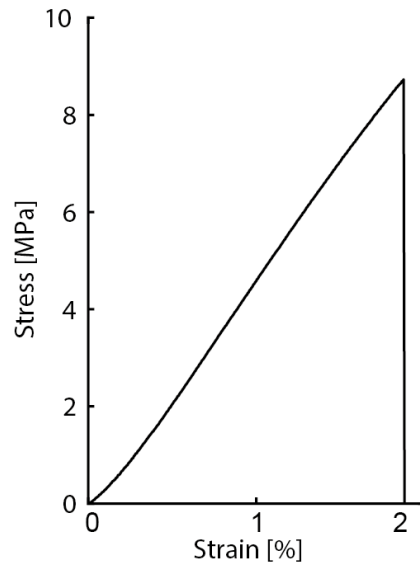


Fig. S7. Mechanical behavior of a representative *Lunaria* septum. The stress-strain curve of a representative *Lunaria* septum is indicative of a strong material with elastic behavior.